Environ. Process. (2015) 2:309–329
DOI 10.1007/s40710-015-0066-6

ORIGINAL ARTICLE

Generalized Quadratic Synaptic Neural Networks for ET_o Modeling

Sirisha Adamala · N. S. Raghuwanshi · Ashok Mishra

Received: 15 October 2014 / Accepted: 16 February 2015 / Published online: 17 March 2015

Abstract This study aims at developing generalized quadratic synaptic neural (GQSN) based reference evapotranspiration (ET_o) models corresponding to the Hargreaves (HG) method. The GQSN models were developed using pooled climate data from different locations under four agro-ecological regions (semi-arid, arid, sub-humid, and humid) in India. The inputs for the development of GQSN models include daily climate data of minimum and maximum air temperatures (T_{min} and T_{max}), extra terrestrial radiation (R_a) and altitude (alt) with different combinations, and the target consists of the FAO-56 Penman Monteith (FAO-56 PM) ET_o. Comparisons of developed GQSN models with the generalized linear synaptic neural (GLSN) models were also made. Based on the comparisons, it is concluded that the GQSN and GLSN models performed better than the HG and calibrated HG (HG-C) methods. Comparison of GQSN and GLSN models, reveal that the GQSN models performed better than the GLSN models for all regions. Both GLSN and GQSN models with the inputs of T_{min}, T_{max} and R_a performed better compared to other combinations. Further, GLSN and GQSN models were applied to locations of model development and model testing to test the generalizing capability. The testing results suggest that the GQSN and GLSN models with the inputs of T_{min}, T_{max} and R_a have a good generalizing capability for all regions.

Keywords Neural networks · Synaptic operation · ANN generalization · Evapotranspiration

1 Introduction

Evapotranspiration (ET) is a key component of the global hydrological cycle and one of the hardest variables to measure among other hydrologic variables (Fisher et al. 2009); it is, therefore of interest to agriculturalists, agronomists, climate modelers, ecologists,

S. Adamala (✉) · N. S. Raghuwanshi · A. Mishra
Agricultural and Food Engineering Department, Indian Institute of Technology, Kharagpur, West Bengal 721302, India
e-mail: sirisha@agfe.iitkgp.ernet.in

N. S. Raghuwanshi
e-mail: nsr@agfe.iitkgp.ernet.in

A. Mishra
e-mail: amishra@agfe.iitkgp.ernet.in

environmentalists, farmers, financiers, hydrologists, and water resources planners/managers. ET is simply the combining process of evaporation and transpiration where water is transferred to the atmosphere in a soil-plant system. Though the evaporation and transpiration are separate processes, they occur simultaneously and difficult to distinguish one from the other (Trajkovic et al. 2003). A common procedure for estimating ET is to first estimate the gross reference evapotranspiration (ET_o) and to then apply an appropriate crop coefficient (k_c).

There exist direct measurement and indirect estimation methods of ET_o. However, direct measurement using lysimeters is cumbersome, time consuming and error-prone. The indirect methods spanning from physically based complex Penman and FAO-56 Penman-Monteith (FAO-56 PM) to radiation or temperature based equations have several limitations. The FAO-56 PM equation, yields the most accurate estimate of ET_o across all climatic conditions when required climate data are available. Although there are several indirect methods, some of them require extended subsets of climatic data and in some of them the complex relationships in between inputs and outputs is difficult to be described analytically. Further, the indirect methods simulate real processes and they must be calibrated with observed climate data. In many cases, the errors in observed climate data are directly transferred to erroneous ET_o estimation. Therefore, the reliability of observed climatic data is essential for better understanding the ET_o process.

To avoid the limitations of existing ET_o models, the artificial neural networks (ANNs) are used in ET_o modeling. Depending upon the order of synaptic operation in a hidden neuron, the ANNs are classified as either first order or higher order (such as second or third or N^{th}) (Gupta et al. 2003). The "first-order neural networks" or "linear synaptic neural (LSN)" models are synonymous to multilayer feed-forward (MLFF) neural networks. Kumar et al. (2011) reviewed thoroughly several ET_o modeling studies using different MLFF and LSN models. Only a few important studies which were not reported there are discussed briefly herein.

Landeras et al. (2008) evaluated seven ANNs to estimate ET_o with different input combinations and compared them with ten locally calibrated empirical and semi-empirical equations. Kim and Kim (2008) proposed a model which combines both the generalized regression neural network (GRNN) and genetic algorithm (GA) to form GRNN-GA model to calculate the pan evaporation (E_p) and the alfalfa reference evapotranspiration (ET_r) with an uncertainty analysis to eliminate the least significant climatic variables. Marti and Gasque (2010) developed temperature-based ANN models through the consideration of exogenous ET_o records as ancillary inputs in different geographical contexts of the Valencia region, and compared them with the existing empirical methods. Marti et al. (2010) described the application of ANNs in estimating ET_o as a function of maximum temperature (T_{max}), minimum temperature (T_{min}), extra terrestrial radiation (R_a), daylight hours, exogenous relative humidity, and ET_o at inland, intermediate, and coastal continental contexts in Spain. The performance of the ANN model was compared with the temperature-based empirical model. Rahimikhoob (2010) examined the potential use of ANNs based on T_{max}, T_{min} and R_a to estimate the ET_o, and compared the ANN estimates with the Hargreaves (HG) and the FAO-56 PM reference model. The HG and calibrated HG (HG-C) significantly under or overestimated and over or underestimated the mean monthly FAO-56 PM ET_o, respectively. Based on these results, local calibration for each site gave acceptable results and this method cannot be recommended for utilization in a regional study. Traore et al. (2010) assessed the performance of MLFF ANN in ET_o modeling based on temperature data, and the ANN models were compared with the HG and FAO-56 PM

methods. Jahanbani and El-Shafie (2011) employed MLFF type ANNs using T_{max},T_{min} and solar radiation (S_{ra}) as input in predicting daily ET_o over a two-month time period. The results showed that the ANN model outperformed the HG method and HG significantly underestimated or overestimated ET_o of FAO-56 PM method.

Kisi (2011) studied the ability of evolutionary neural networks (ENN) to model ET_o using daily climatic data as inputs. A comparison was made between the estimates provided by the ENN and those of the following empirical models: California Irrigation Management Information System (CIMIS), Penman, HG, modified HG, and Ritchie methods and the conventional ANN. Huo et al. (2012) modeled and compared ANNs with the multi-linear regression (MLR) models, Penman, and with two empirical models for estimating ET_o as a function of 50-year climatic data. Laaboudi et al. (2012) examined the effectiveness of the ANNs in the evaluation of daily ET_o using incomplete meteorological parameters (air temperature, relative humidity (RH), wind speed (W_s), and the insolation duration) as inputs. El-Shafie et al. (2013) developed both the ANN and auto-regression moving average (ARMA) based monthly ET_o models, and compared them with the HG method. Shiri et al. (2013) evaluated the capabilities of generalized neuro-fuzzy (GNF) models in estimating ET_o using two separate sets of weather data from humid and non-humid regions of Spain and Iran. The GNF models were trained using data from Spanish humid and non-humid regions and tested in Iranian humid and non-humid stations, respectively. Further, a global GNF model was trained by considering pooled data of all Spanish stations and tested in Iran. Adamala et al. (2014a) developed second order neural network based ET_o models corresponding to FAO-56 PM method for different climatic locations in India. The authors compared the performance of the developed models with the MLFF models. Adamala et al. (2014b) tested the generalizing capability of higher-order neural networks corresponding to four conventional ET_o estimation methods. Falamarzi et al. (2014) utilized the ANN and wavelet neural network (WNN) models to forecast daily ET_o from T_{max}, T_{min} and W_s data as inputs, and FAO-56 PM ET_o as output. Shiri et al. (2014) evaluated the generalizability of gene expression programming (GEP) based ET_o models through spatial and temporal k-fold testing in a coastal environment in Iran. Chen et al. (2015) investigated the transferability of support vector machines (SVM) in the estimation of solar radiation in subtropical zone in China.

All the above cited studies used the MLFF or LSN neural networks to model ET_o. These neural networks are able to extract the first-order or linear correlations that exist between input and the synaptic weight vectors. However, the climatic variables associated with ET_o exhibit high non-linearity during modeling and these LSN models fail to extract the complete non-linearity that is present in the data because of linear synaptic operation. To overcome the above limitation that is associated with the LSN models, many researchers have focused on using quadratic synaptic neural (QSN) models which employ a second order synaptic operation between inputs and synaptic weights to extract non-linear correlations (Chakra et al. 2013). The QSN models are capable of capturing not only the first order correlations but also the second-order correlations that exist between the components of the input patterns. This property makes QSN models superior as compared to the LSN models.

One limitation associated with the LSN and QSN models is their lack of generalizing capability because they are applicable to data from the locations which are used in training or model development (these locations are indicated as 'model development locations'). When new location data, i.e., data from locations that were not used during the model development (these locations are represented as 'model test locations') are introduced to the developed network, the network fails to provide good performance, indicating poor generalizing capacity. This limitation can be overcome by developing generalized LSN (GLSN) and generalized (GQSN) models which not only perform well for model development locations but also for model test locations. This can be achieved by

considering pooled climatic data of various locations which have properties of both spatial and altitudinal variations during model development.

In a developing country like India, with significant spatial variation in climate, the required climatic data for ET_o estimation may be difficult to be obtained at every location. The most readily available data for India may be the T_{max} and T_{min}. This shows the need of developing GQSN models with minimum available climatic input data for ET_o estimation. Further, the development of GQSN models involves the pooling of climatic data from different locations. Therefore, consideration of only T_{max} and T_{min} input data for a number of pooled locations may not improve the generalizing capability as the latitude (lat) and altitude (alt) from one location to another location vary significantly. Instead of directly using 'lat' as input variable, the latitude is compensated by the R_a in HG equation. Therefore, the objectives of this study are formulated as:

1. To develop GQSN models for the estimation of ET_o for different agro-ecological regions (AERs) of India.
2. To compare the developed GQSN models with the GLSN models.
3. To test the generalizing capability of GQSN and GLSN models to model development and model testing locations.

2 Materials and Methods

2.1 Study Area and Climate Data

The climatic data that was used in to this study were collected from All India Coordinated Research Project on Agro-meteorology (AICRPAM), Central Research Institute for Dryland Agriculture (CRIDA), Hyderabad, Andhra Pradesh, India. The data included all the parameters that are required for the calculation of ET_o by the FAO-56 PM method, but only a subsample of the data that included daily T_{min} and T_{max} values was used for the development and testing of the ANNs. This practice simulated conditions of limited input data for the ANNs. The R_a was calculated from Hargreaves and Samani (1985) equation. Because of the unavailability of measured lysimeter ET_o data for the selected study locations, ET_o was estimated by the FAO-56 PM method which is considered as the method for the computation of ET_o in the absence of lysimeter data (Allen et al. 1998). The data that was used in this work was collected by 25 climatic stations that were distributed over four AERs: semi-arid, arid, sub-humid, and humid. Figure 1 shows the geographical locations of the selected stations and their related AERs. Table 1 presents information related to altitude, observation periods, and statistical summary of the FAO-56 PM ET_o for the chosen locations. The altitude of selected locations varied from 10 m at Mohanpur to 1600 m at Ranichauri above mean sea level. The parameters $ET_{o_{mean}}$ and σ_{ET_o} denote mean and standard deviation of ET_o, respectively. The mean (time-averaged) value of ET_o varied between a minimum of 2.87 mm day^{-1} at the sub-humid region of RN and a maximum of 6.13 mm day^{-1} at the arid region of AT. The minimum and maximum standard deviations of ET_o were observed in the humid region of DP (1.0 mm day^{-1}) and the semi-arid region of AK (2.56 mm day^{-1}), respectively. Figure 2 shows the variation of mean daily FAO-56 PM ET_o and climatic data of T_{max} and T_{min} for 25 locations. The highest and lowest mean (time-averaged) values of T_{max} were observed at a semi-arid region of KV and sub-humid region of RN locations, respectively. Similarly, the maximum and minimum mean (time-averaged) values of T_{min} occurred at a humid region of TH and sub-humid region of RN locations, respectively.

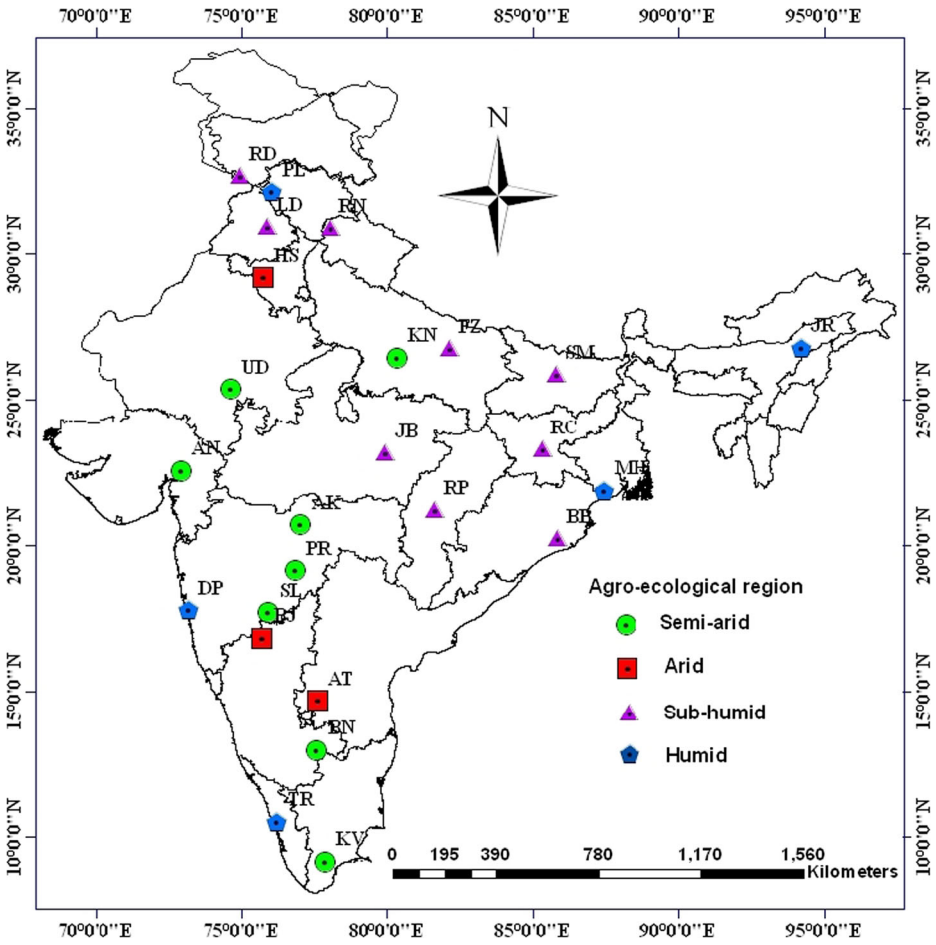

Fig. 1 Geographical locations of study sites in India

2.2 Generalized Artificial Neural Network (GANN) Models

The GANNs consist of the conventional neural units (NU) which provide the neural output as a nonlinear function of the linear combination of the weighted neural inputs. Generally, GANNs are represented as parallel distributed units with a crucial ability of learning and adaptation. The architecture of the GANN models is accomplished by capturing the higher-order association as well as the linear association between the elements of the input patterns. The higher-order weighted combination of the inputs will yield higher neural performance as they require fewer training passes and a smaller training set to achieve the generalization over the input domain. But for complex hydrologic variables, there may exist some of the nonlinear correlations also. GANNs have good computational, storage, and learning properties due to their ability to exploit the cross- and self-correlations between the inputs (Taylor and Commbes 1993). Therefore, to extract higher order correlations with a good learning capability, these GANNs can be used as an efficient tool.

Generally, GANNs are categorized as GLSN and GQSN models based on the type of synaptic operation. The processing of information in any biological or artificial

Table 1 Characteristics and summary statistics of daily FAO-56 PM ET_o for the study locations

Location	Index	Alt. (m)	Role	Period	$ET_{o_{mean}}$ (mm day^{-1})	σ_{ET_o} (mm day^{-1})
Semi-arid						
Parbhani	PR	423	Tr, V, Ts	2001–2005	4.84	1.68
Solapur	SL	25	Tr, V, Ts	2001–2005	4.83	1.51
Bangalore	BN	930	Tr, V, Ts	2001–2005	4.47	1.10
Kovilpatti	KV	90	Tr, V, Ts	2001–2005	5.32	1.66
Udaipur	UD	433	Tr, V, Ts	2001–2005	4.20	1.83
Kanpur	KN	126	Ts	2004–2005	4.06	1.93
Anand	AN	45	Ts	2002–2005	4.20	1.45
Akola	AK	482	Ts	2001–2003	5.25	2.56
Arid						
Anantapur	AT	350	Tr, V, Ts	2001–2005	6.13	1.82
Hissar	HS	215	Tr, V, Ts	2001–2005	4.21	2.12
Bijapur	BJ	594	Ts	2001–2004	4.42	1.26
Sub-humid						
Raipur	RP	298	Tr, V, Ts	2001–2005	4.31	1.87
Faizabad	FZ	133	Tr, V, Ts	2001–2005	3.77	1.65
Ludhiana	LD	247	Tr, V, Ts	2001–2005	3.91	1.98
Ranichauri	RN	1600	Tr, V, Ts	2001–2005	2.87	1.25
Jabalpur	JB	393	Ts	2002–2005	3.92	1.69
Samastipur	SM	52	Ts	2004–2005	3.85	1.58
Bhubaneshwar	BB	25	Ts	2002–2005	4.37	1.57
Ranchi	RC	625	Ts	2005	3.46	1.29
Rakh Dhiansar	RD	332	Ts	2005	3.07	1.61
Humid						
Palampur	PL	1291	Tr, V, Ts	2001–2005	3.43	1.48
Jorhat	JR	86	Tr, V, Ts	2001–2005	2.90	1.01
Mohanpur	MH	10	Tr, V, Ts	2001–2005	3.60	1.24
Dapoli	DP	250	Tr, V, Ts	2001–2005	3.65	1.00
Thrissur	TR	26	Ts	2001–2004	4.27	1.27

Tr train, *V* validation, *Ts* test

neural models involves two distinct operations: (a) synaptic operation; and (b) somatic operation. In synaptic operation, different weights are assigned to each input matrix based on past experience or knowledge with an addition of bias or threshold (Fig. 3). In somatic operation, the synaptic output is applied to a nonlinear activation function (ϕ) (Tiwari et al. 2012). Mathematical representation of synaptic and somatic operations in a neural network is shown in Eqs. (1) and (2), respectively.

$$y = \sum_{i=0}^{n} w_i x_i = w_0 x_0 + w_1 x_1 + \ldots + w_n x_n \tag{1}$$

$$z = \phi[y] \tag{2}$$

where

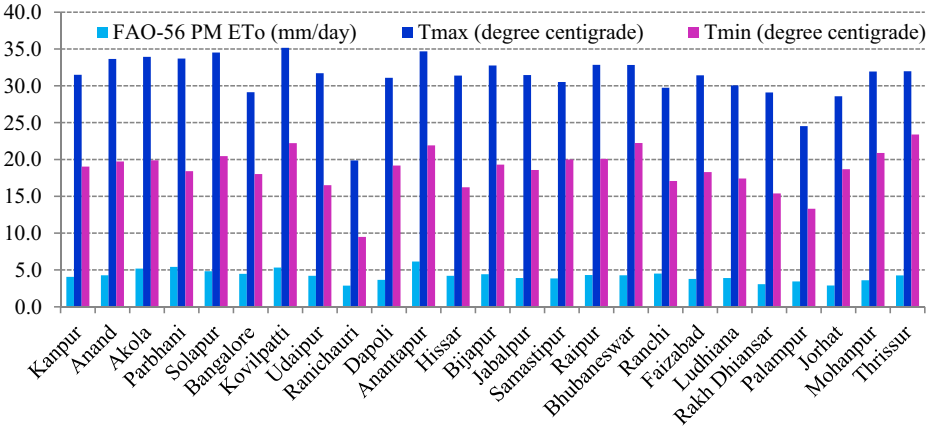

Fig. 2 Station wise variation of mean daily FAO-56 PM ET_o, T_{max} and T_{min}

y neural synaptic output
z neural somatic output
w_0 threshold weight
x_0 constant bias (=1)
x_i neural inputs at the i^{th} step
w_i synaptic weights at the i^{th} step
ϕ activation function (sigmoidal)
n number of elements in the input vector.

2.2.1 Generalized Linear Synaptic Neural (GLSN) Model

The GLSN model provides the neural output as a nonlinear function of the weighted linear combination of the neural inputs. In GLSN model, the synaptic operation is of the first order which

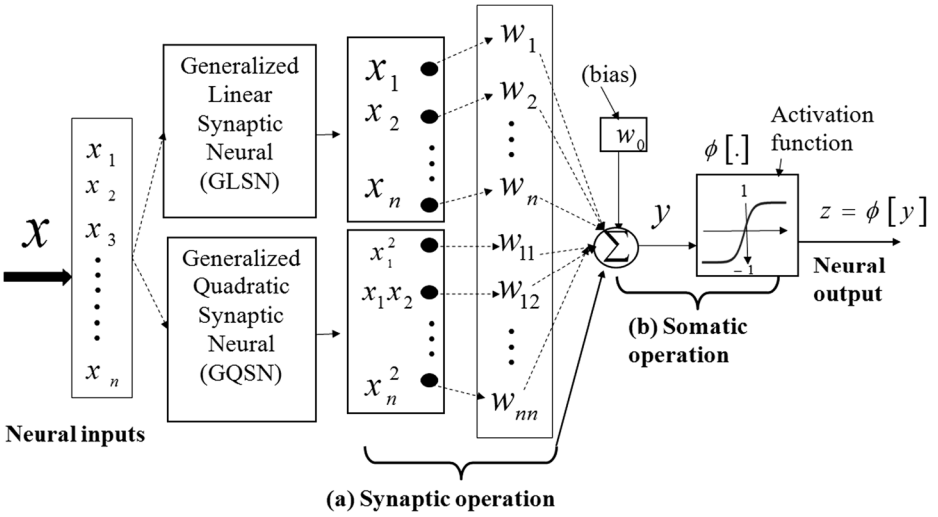

Fig. 3 Architecture of generalized synaptic neural network models

means that only first order correlations exist between the inputs and the synaptic weights of the model. Let N and n be the order and the number of inputs to the neuron, respectively. For N=1, the mathematical expression of GLSN model is given as (Redlapalli 2004):

$$(z)_{N=1} = \phi\left(\sum_{i_1=0}^{n} w_{i_1} x_{i_1}\right) \tag{3}$$

where

x_{i_1} neural inputs at the i_1^{th} step
w_{i_1} synaptic weights at the i_1^{th} step.

2.2.2 Generalized Quadratic Synaptic Neural (GQSN) Model

The synaptic operation of the GQSN embraces both the first and second-order neural input combinations with the synaptic weights. In GQSN model, the synaptic operation in a neural unit or a node is of the second order which means that there exist not only first order but also second order correlations with second order terms between inputs and synaptic weights. For N=2, the mathematical model of GQSN is represented as (Redlapalli 2004):

$$(z)_{N=2} = \phi\left(\sum_{i_1=0}^{n}\sum_{i_2=i_1}^{n} w_{i_1 i_2} x_{i_1} x_{i_2}\right) \tag{4}$$

where

x_{i_2} neural inputs at the i_2^{th} step
$w_{i_1 i_2}$ synaptic weights at the $i_1 i_2^{\text{th}}$ step.

2.3 Conventional Evapotranspiration Computation Methods

The HG method uses only temperature and latitude data for estimating ET_o. The Hargreaves equation is one of the simplest equations used to estimate ET_o. It is expressed as (Hargreaves and Samani 1985):

$$ET_o = 0.0023 R_a \sqrt{TD}\left(T_{avg} + 17.8\right) \tag{5}$$

where

ET_o reference evapotranspiration (mm day^{-1})
T_{max} maximum daily air temperature at 2 m height (°C)
T_{min} minimum daily air temperature at 2 m height (°C)
TD difference between T_{max} and T_{min} (°C) at 2 m height
R_a extraterrestrial solar radiation (function of latitude and day of the year) (MJ m^{-2} day^{-1})
T_{avg} average daily air temperature at 2 m height (°C).

The calibrated HG (HG-C) equation is developed by calibrating the HG equation with reference to standard FAO-56 PM equation for a particular location. FAO of the

United Nations accepted the FAO-56 PM method as a standard equation for the estimation of ET_o and the evaluation of other methods (Allen et al. 1998):

$$ET_o = \frac{0.408\Delta(R_n - G) + \gamma \frac{900}{T_{avg} + 273} W_s(e_s - e_a)}{\Delta + \gamma(1 + 0.34W_s)} \quad (6)$$

where

R_n daily net solar radiation (MJ m^{-2} day^{-1})
G soil heat flux (MJ m^{-2} day^{-1})
e_s saturation vapor pressure (kPa)
e_a actual vapor pressure (kPa)
Δ slope of saturation vapor pressure versus air temperature curve (kPa $°C^{-1}$)
W_s wind speed at 2 m height (m s^{-1})
γ psychrometric constant (kPa $°C^{-1}$).

2.4 Data Preparation

For the development of GLSN and GQSN models for different AERs, locations having daily data for the period 2001–2005 were chosen. The data were divided into training sets (denoted as Tr and used to adjust the weights and biases during learning), validation sets (denoted as V and used to avoid overfitting), and testing sets (denoted as Ts and used to predict with new data). The locations with 'Tr, V, Ts' role (Table 1) were used to develop GLSN and GQSN models (model development locations). These locations for model development were selected because of the availability of a larger set of data during the study period as compared to other locations. In this study, the habitual practice of using a standard holdout strategy for dividing the data was followed as it is a very common practice in hydrological modeling. For these locations, 70 and 30 % of data for the period 2001–2004 were used for training and validation, respectively. It would be more complicated to use different year of dataset for different locations. Therefore, the same 2005 year data was used for testing the performance of developed models. However, the data for the same testing (2005) year have different complexity considering the different agro-climatic zones.

The data were pooled from (PR, SL, BN, KV, and UD), (AT and HS), (RP, FZ, LD, and RN), and (PL, JR, MH, and DP) locations (Table 1) to develop GLSN and GQSN models for semi-arid, arid, sub-humid, and humid regions, respectively. To test the generalizing capability of the developed models (either for practical application or just for testing purposes), these models were applied to data from the locations that were not used during model development. The locations with only 'Ts' role (Table 1) were used to test the generalizing capability of the developed models (model testing locations). As an example, for the locations that lie in semi-arid regions (PR, SL, BN, KV, and UD) the pooled data of 2001–2004 were used to train (including validation) the GLSN and GQSN models, while the data of 2005 were used to test these models. The generalizing capability of GLSN and GQSN models was tested using data from locations (KN, AN, and AK) that were not included during development in semi-arid region. In a similar way, different GLSN and GQSN models were developed and tested for their generalization capabilities in arid, sub-humid, and humid regions. The outlined methodology for developing both the GLSN and GQSN models is shown in Fig. 4.

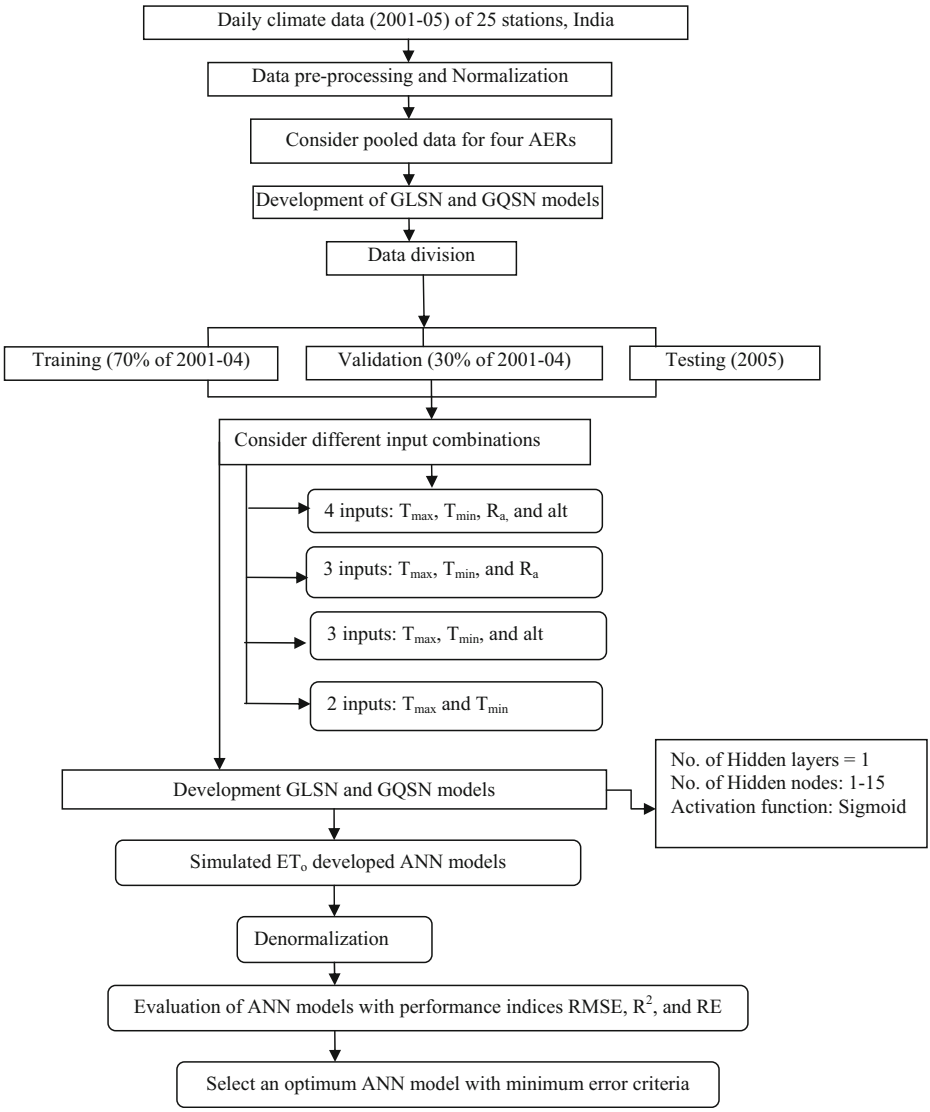

Fig. 4 Methodology for developing both the GLSN and GQSN models

2.5 Criteria for Preprocessing and Estimation of Parameters

As a first step in developing GLSN and GQSN models, normalization before presenting data as input to network and denormalization after developing optimum network were performed using a Matlab built-in function called 'mapstd' which rescales data so that their mean and standard deviation become equal to 0 and 1, respectively. The inputs for developing GLSN and GQSN models include T_{max}, T_{min}, R_a and alt. This study examined four combinations of these inputs to both models. Thus, the sensitivity of ET_o on each of these variables was evaluated. Accordingly, the input combinations evaluated in the present study are: (i) T_{max}, T_{min}, R_a and alt; (ii) T_{max}, T_{min}

and R_a; (iii) T_{max}, T_{min} and alt; and (iv) T_{max} and T_{min}. The target consists of the daily value of ET_o obtained by the FAO-56 PM equation. Only one hidden layer was used in both the GLSN and GQSN models, as it is enough for the representation of the non-linear relationship between climate variables and ET_o (Kumar et al. 2002).

The important parameters for network training are the learning rate, which tends towards a fast, steepest-descent convergence, and the momentum, a long-range function preventing the solution from being trapped into local minima. The other parameters are activation function, error function, learning rule, and initial weight distribution (i.e., initialization of weights). Table 2 shows the calibrated parameters of developed models. Sigmoidal activation function was employed in the output layer neurons. Figure 5 illustrates a plot for finding the optimum number of hidden nodes for both GLSN and GQSN models. The optimum number of hidden nodes was found to be i+1 (where i = number of nodes in the input layer) and 2 for GLSN and GQSN models, respectively, after several trial and error experiments with 1 to 15 hidden nodes based on minimum RMSE and maximum R^2 criteria (Adamala et al. 2014a). The threshold RMSE error was set at 0.0001. A learning rate and momentum rate of 0.65 and 0.5, respectively, were fixed for the selected network after several trials. The network training was continued until the threshold RMSE error was reached and was found to stop after approximately 500 epochs with the range of possible numbers of epochs extending from 100 to 1000. For developing GQSN based daily ET_o models, the code was written using Matlab 7.0 programming language.

2.6 Performance Evaluation

The performance evaluation of all the developed models is carried out for both the training, validation and testing periods in order to examine their effectiveness in simulating ET_o. The performance indices used in evaluating the models are the: root mean squared error (RMSE, mm day^{-1}), relative error (RE), and coefficient of determination (R^2, dimensionless). A description of the aforementioned indices is provided below.

$$\mathrm{RMSE} = \sqrt{\frac{1}{n}\sum_{i=1}^{n}\left(T_i - O_i\right)^2} \tag{7}$$

Table 2 Calibration parameters of developed models

Calibrated parameters	Trial range	Optimum values
Learning rate	0.1 to 0.9 with a step of 0.05	0.65
Momentum	0.1 to 0.9 with a step of 0.1	0.5
Hidden node numbers	1 to 15	i+1 for GLSN and 2 for GQSN models
No. of epochs	100 to 1000 at a step of 100	500
Threshold RMSE error	Set at 0.0001	0.0001
Activation function	Sigmoidal	Sigmoidal

i = number of nodes in the input layer

$$R^2 = \frac{\left[\sum_{i=1}^{n}\left(O_i - \overline{O}\right)\left(T_i - \overline{T}\right)\right]^2}{\sum_{i=1}^{n}\left(O_i - \overline{O}\right)^2 \sum_{i=1}^{n}\left(T_i - \overline{T}\right)^2} \tag{8}$$

$$RE = \sum_{i=1}^{n} \frac{|T_i - O_i|}{T_i} \tag{9}$$

where

T_i and O_i	target (FAO-56 PM ET_o) and output (ET_o predictions of the GLSN and GQSN models) values at the i^{th} step, respectively
n	number of data points
$\overline{T}$ and $\overline{O}$	average of target and output values, respectively.

3 Results and Discussion

As per the above mentioned criteria in Section 2.5, the GLSN and GQSN models were trained and the optimum parameters were found after a number of trials. This section presents the best results of GLSN and GQSN models corresponding to HG conventional ET_o method in four AERs.

3.1 Simulation Results of Developed Models

Table 3 shows the performance of GLSN and GQSN models (with four input combinations) in terms of RMSE, R^2, and RE in different AERs. The GQSN models were compared with the GLSN models to test the relative performance of quadratic (second order) over linear (first order) neural models. Table 3 indicates that the GQSN model whose inputs are T_{max}, T_{min}, R_a and alt (input combination (i)) performed better with the smallest RMSE (mm day^{-1}) values of 0.635, 0.775, 0.647 and 0.618, and the highest R^2 values of 0.847, 0.870, 0.878 and 0.773 for

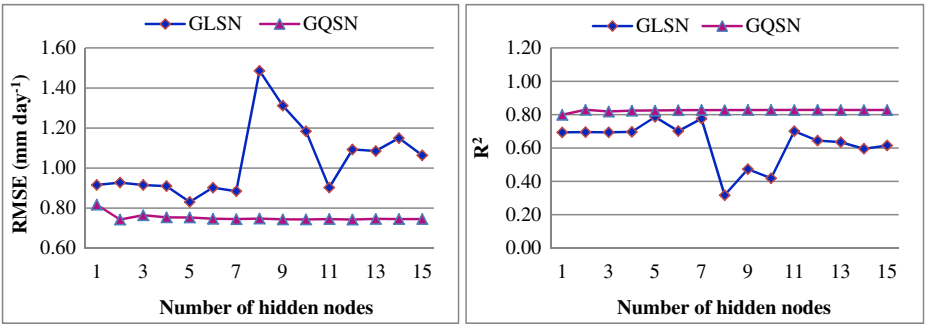

Fig. 5 Trend of RMSE and R^2 with the number of hidden nodes for GLSN and GQSN models

Table 3 Performance statistics of neural models during model development (2005 year pooled data)

AER	Input	GLSN			GQSN			HG			HG-C		
		RMSE	R^2	RE	RMSE	R^2	RE	RMSE	R^2	RE	RMSE	R^2	RE
Semi-arid	(i)	0.653	0.839	0.114	0.635	0.847	0.109	0.962	0.776	0.165	0.767	0.776	0.143
	(ii)	0.682	0.825	0.119	0.668	0.830	0.117						
	(iii)	0.721	0.803	0.132	0.704	0.811	0.130						
	(iv)	0.836	0.736	0.156	0.817	0.746	0.152						
Arid	(i)	0.838	0.847	0.126	0.775	0.870	0.115	1.247	0.685	0.192	1.452	0.665	0.232
	(ii)	0.939	0.808	0.144	0.894	0.825	0.137						
	(iii)	1.023	0.771	0.152	0.911	0.820	0.137						
	(iv)	1.093	0.739	0.171	1.055	0.759	0.167						
Sub-humid	(i)	0.658	0.873	0.115	0.647	0.878	0.112	1.058	0.812	0.191	1.510	0.812	0.258
	(ii)	0.671	0.869	0.118	0.663	0.872	0.119						
	(iii)	0.722	0.846	0.139	0.722	0.847	0.139						
	(iv)	0.749	0.829	0.141	0.735	0.837	0.132						
Humid	(i)	0.629	0.764	0.151	0.618	0.773	0.149	0.959	0.724	0.199	1.379	0.724	0.276
	(ii)	0.663	0.739	0.159	0.646	0.754	0.156						
	(iii)	0.672	0.734	0.161	0.658	0.742	0.158						
	(iv)	0.852	0.575	0.209	0.842	0.582	0.206						

Input combinations (i) T_{max}, T_{min}, R_a, and alt; (ii) T_{max}, T_{min}, and R_a; (iii) T_{max}, T_{min}, and alt; (iv) T_{max} and T_{min}

semi-arid, arid, sub-humid and humid regions, respectively. The RE values of GQSN models were 0.109, 0.115, 0.112 and 0.149 for semi-arid, arid, sub-humid and humid regions, respectively. The GLSN model with input combination (i) is the second better model with the RMSE (mm day^{-1}) values of 0.653, 0.838, 0.658 and 0.629 for semi-arid, arid, sub-humid and humid regions, respectively (Table 3). The GQSN model with input combination (iv), which has only T_{max} and T_{min} as input, had the worst performance with RMSE (mm day^{-1}) values 0.817, 1.055, 0.735 and 0.842 for semi-arid, arid, sub-humid and humid regions, respectively. The performance of GLSN model with input combination (iv) showed RMSE (mm day^{-1}) values of 0.836, 1.093, 0.749 and 0.852 for semi-arid, arid, sub-humid and humid regions, respectively. Similarly, the RMSE values of GLSN were slightly higher compared to GQSN model RMSE values for the input combinations (ii) and (iii) in four AERs.

This confirms the better performance of GQSN models over GLSN models. The reason for this superior performance of the GQSN models over the GLSN models is probably their capability to capture non-linearity, as the GQSN models use non-linear approximation functions with second order polynomials (Eq. 4). Further, the models with the input combination (i) performed better compared to models of other combinations. The GLSN and GQSN models with the input combination (i) performed approximately 5, 10, and 20 % superior compared to the input combinations (ii), (iii) and (iv), respectively, for all AERs. The reason for this superior performance might be due to the inclusion of alt and R_a data as inputs which may have great influence on generalized models as these were developed using data from different locations. The performance of the GLSN and GQSN models was decreased by 5 and 10 %, for models developed without considering alt and R_a. This shows the importance of altitude in modeling generalized models as it varies from one location to other location very much (Table 1). The R_a is a function of latitude, which is also a very important parameter that should be considered as GLSN and GQSN models were developed with the pooled data of many locations in different AERs during the development of generalized models.

The GQSN and GLSN models were further compared with the HG and HG-C method, to check the superiority of ANN (GLSN and GQSN) models over conventional methods (Table 3). The RMSE (mm day^{-1}) values of the HG method were 0.962, 1.247, 1.058 and 0.959 for semi-arid, arid, sub-humid and humid regions, respectively. The HG-C model yielded RMSE (mm day^{-1}) values of 0.767, 1.452, 1.510 and 1.379 for semi-arid, arid, sub-humid and humid regions, respectively. This statistic confirms the greater RMSE values of HG and HG-C methods compared to the GLSN and GQSN models. Therefore, it is feasible to use ANNs in modeling ET_o.

Figure 6 shows the scatter plots of the predictions of developed GLSN, GQSN models and HG and HG-C estimated ET_o with respect to the FAO-56 PM in four AERs. Due to the superior performance of GQSN and GLSN models with input combination (i) over the other combinations, the scatter plots were drawn only for these models corresponding to four AERs and are shown in Fig. 6 which confirms the statistics given in Table 3. Figure 6 results illustrate that the agreement between the ET_o predictions of the GQSN models and the FAO-56 PM ET_o predictions was better for all regions. The GQSN models, result in R^2 values>0.847 in all regions except for the humid region (R^2=0.773). The reason for this worse performance of the GQSN models in humid regions might be the absence of relative humidity as an input during model development, because humidity is an important variable in humid regions. The simple linear regression equations ($y = a_0x + a_1$) are also presented in the figure. The fit line equations in Fig. 6 gave the values of a_0 and a_1 coefficients close to one and zero, respectively. Comparison of GLSN and GQSN plots with the HG and HG-C models reveals that the spread of HG and HG-C estimated ET_o around the 1:1 line is less than that of the GLSN and GQSN estimated ET_o. The GLSN and GQSN models linearly fit on 1:1 line more perfectly than

the HG and HG-C models. It can be clearly seen that the values of GLSN and GQSN models are denser in the neighborhood of the linear 1:1 line.

Figure 7 shows the scatter plots of developed GLSN and GQSN models with respect to the FAO-56 PM in four AERs with an input combination of T_{max}, T_{min} and R_a. Similarly to Fig. 6, the distributions of the ET_o predictions of the GQSN models were slightly better than the distributions of the ET_o predictions of the GLSN models in Fig. 7. These scatter plots confirm the statistics given in Table 3 for four AERs. Regression analysis was performed between the FAO-56 PM ET_o and ET_o estimated with the GLSN and GQSN models and the best-fit lines are shown in Fig. 7. The values of R^2 for GLSN and GQSN models were found to be >0.739 and >0.754, respectively. The fit line equations ($y = a_0x + a_1$) in Fig. 7 gave the values of a_0 and a_1 coefficients close to one and zero, respectively.

3.2 Generalization of GLSN and GQSN Models

In order to study the generalizing capability of the developed GLSN and GQSN models for different regions, these models were tested under two different scenarios: (a) with data of year 2005 from locations that were used during model development (model development locations); and (b) with new data from locations that were not used during model development (model testing locations). Tables 4, 5 and 6 show the performance statistics in terms of RMSE, R^2 and RE, respectively, of GLSN and GQSN models with individual location data under scenario (a) for different AERs. For example, in the semi-arid region, the GLSN and GQSN models were tested in five locations, namely PR, SL, BN, KV, and UD (2005 year data for each individual location). Similarly, GQSN models

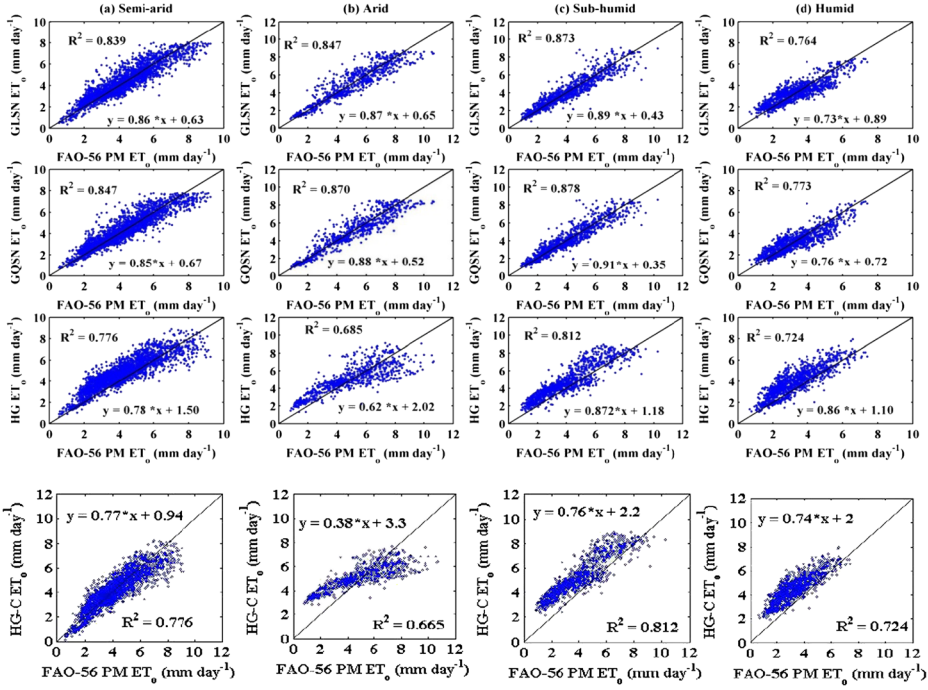

Fig. 6 Scatter plots of GLSN, GQSN, HG, and HG-C methods with respect to the FAO-56 PM for different AERs with an input combination of T_{max}, T_{min} R_a, and alt

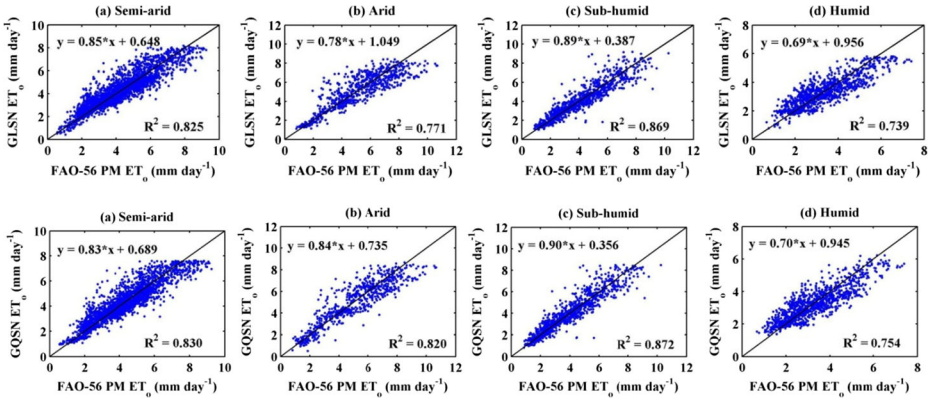

Fig. 7 Scatter plots of GLSN and GQSN models with respect to the FAO-56 PM for different AERs with an input combination of T_{max}, T_{min} and R_a

were tested with AT and HS (arid), RP, FZ, LD, and RN (sub-humid), and PL, JR, MH, and DP (humid) location data. For all the above cases, the performance of GQSN models with input combination (ii) was superior compared to other combinations. Further, the GQSN models showed slightly better generalization compared to GLSN models. The GLSN and GQSN models with input combinations (i) and (iii) failed to show generalizing capability, as these models showed higher RMSE and very low R^2 values compared to other combinations (ii) and (iv). Both models with these

Table 4 Performance statistics in terms of RMSE of generalized models with model development locations

AER	Location	RMSE (mm day^{-1})									
		(i)		(ii)		(iii)		(iv)		HG	HG-C
		GLSN	GQSN	GLSN	GQSN	GLSN	GQSN	GLSN	GQSN		
Semi-arid	PR	1.817	1.776	0.649	0.619	2.769	2.312	0.726	0.706	1.059	1.705
	SL	1.607	1.610	0.708	0.696	2.639	2.376	0.750	0.744	1.001	1.465
	BN	2.990	2.646	0.664	0.646	2.181	1.941	0.804	0.706	0.964	0.653
	KV	3.396	3.631	1.006	0.976	2.663	2.293	1.081	1.026	1.128	1.431
	UD	2.122	1.910	0.785	0.745	2.634	2.135	0.896	0.864	1.078	1.448
Arid	AT	2.173	1.530	1.014	0.973	2.724	2.236	1.164	1.046	1.350	1.704
	HS	2.368	1.756	0.839	0.753	2.967	2.436	0.957	0.928	1.134	1.723
Sub-humid	RP	2.220	2.085	0.693	0.649	2.025	1.753	0.797	0.711	0.998	1.505
	FZ	1.973	1.341	0.623	0.615	1.921	1.787	0.684	0.673	1.259	2.016
	LD	2.324	1.757	0.659	0.653	2.327	2.041	0.799	0.791	0.881	1.161
	RN	2.585	2.172	0.602	0.585	2.627	2.315	0.746	0.725	0.880	0.832
Humid	PL	2.936	2.114	0.652	0.647	2.971	2.605	0.791	0.759	0.861	0.787
	JR	2.605	1.522	0.706	0.686	2.760	2.092	0.734	0.712	1.015	1.331
	MH	2.713	1.938	0.647	0.590	2.497	2.265	0.707	0.687	1.137	1.857
	DP	2.868	2.537	0.621	0.592	2.092	1.861	0.749	0.742	1.129	1.813

Input combinations—(i) T_{max}, T_{min}, R_a, and alt; (ii) T_{max}, T_{min}, and R_a; (iii) T_{max}, T_{min}, and alt; (iv) T_{max} and T_{min}

Table 5 Performance statistics in terms of R^2 of generalized models with model development locations

AER	Location	R^2									
		(i)		(ii)		(iii)		(iv)		HG	HG-C
		GLSN	GQSN	GLSN	GQSN	GLSN	GQSN	GLSN	GQSN		
Semi-arid	PR	0.128	0.146	0.866	0.868	0.108	0.115	0.810	0.823	0.738	0.838
	SL	0.260	0.277	0.820	0.830	0.157	0.186	0.776	0.787	0.683	0.783
	BN	0.365	0.386	0.702	0.719	0.169	0.196	0.597	0.626	0.569	0.769
	KV	0.277	0.281	0.624	0.637	0.132	0.146	0.539	0.574	0.517	0.587
	UD	0.243	0.279	0.831	0.856	0.146	0.170	0.772	0.793	0.676	0.776
Arid	AT	0.489	0.511	0.680	0.721	0.133	0.152	0.640	0.678	0.575	0.575
	HS	0.386	0.496	0.822	0.860	0.113	0.133	0.774	0.790	0.645	0.845
Sub-humid	RP	0.162	0.186	0.875	0.897	0.179	0.205	0.840	0.867	0.830	0.829
	FZ	0.302	0.396	0.870	0.874	0.245	0.265	0.843	0.847	0.792	0.792
	LD	0.269	0.302	0.897	0.897	0.146	0.154	0.846	0.849	0.757	0.857
	RN	0.196	0.219	0.877	0.884	0.124	0.148	0.712	0.732	0.691	0.891
Humid	PL	0.211	0.245	0.742	0.797	0.193	0.206	0.692	0.725	0.632	0.832
	JR	0.267	0.325	0.547	0.558	0.232	0.257	0.511	0.516	0.494	0.511
	MH	0.146	0.255	0.765	0.796	0.130	0.145	0.721	0.748	0.502	0.802
	DP	0.154	0.185	0.743	0.764	0.125	0.155	0.580	0.602	0.483	0.683

Input combinations—(i) T_{max}, T_{min}, R_a, and alt; (ii) T_{max}, T_{min}, and R_a; (iii) T_{max}, T_{min}, and alt; (iv) T_{max} and T_{min}

Table 6 Performance statistics in terms of RE of generalized models with model development locations

AER	Location	RE									
		(i)		(ii)		(iii)		(iv)		HG	HG-C
		GLSN	GQSN	GLSN	GQSN	GLSN	GQSN	GLSN	GQSN		
Semi-arid	PR	0.283	0.227	0.102	0.098	0.353	0.321	1.203	0.119	0.168	0.255
	SL	0.259	0.217	0.114	0.112	0.346	0.291	1.293	0.122	0.159	0.226
	BN	0.387	0.354	0.128	0.112	0.302	0.275	0.144	0.132	0.098	0.114
	KV	0.401	0.398	0.173	0.150	0.321	0.312	0.172	0.161	0.174	0.211
	UD	0.353	0.287	0.178	0.132	0.546	0.421	0.171	0.163	0.192	0.249
Arid	AT	0.245	0.167	0.198	0.131	0.281	0.249	0.160	0.141	0.191	0.267
	HS	0.365	0.289	0.153	0.134	0.401	0.378	0.186	0.179	0.195	0.283
Sub-humid	RP	0.761	0.678	0.129	0.112	0.456	0.344	0.631	0.609	0.177	0.251
	FZ	0.891	0.795	0.120	0.101	0.406	0.373	0.142	0.123	0.225	0.325
	LD	1.134	1.038	0.114	0.113	0.678	0.449	0.155	0.145	0.169	0.216
	RN	0.608	0.509	0.153	0.137	0.463	0.439	0.205	0.197	0.133	0.201
Humid	PL	0.457	0.394	0.198	0.162	0.446	0.435	0.560	0.548	0.141	0.165
	JR	0.389	0.324	0.204	0.182	0.469	0.391	0.201	0.184	0.231	0.291
	MH	0.621	0.547	0.145	0.128	0.379	0.359	0.163	0.154	0.220	0.328
	DP	0.426	0.391	0.151	0.142	0.338	0.314	0.179	0.177	0.220	0.322

Input combinations—(i) T_{max}, T_{min}, R_a, and alt; (ii) T_{max}, T_{min}, and R_a; (iii) T_{max}, T_{min}, and alt; (iv) T_{max} and T_{min}

combinations (i) and (iii) showed worse performance even when compared to the model. For example, in the semi-arid region, the GLSN and GQSN models when compared to the model with the combination (iv) which has inputs of T_{max} and T_{min} and the conventional HG method. In both combinations (i) and (iii), the altitude of different locations was included as an input variable. Therefore, these results show that the consideration of altitude is not necessary while testing generalizing capability of ANN models, as the altitude forces the models to show worst performance. Because of this, the generalizing capability was lost during testing. These results imply that in scenario (a) the performance of both the GQSN and GLSN models with (ii) and (iv) input combinations showed good generalization for all locations under four AERs.

Table 7 illustrates the performance statistics of GLSN and GQSN models with model testing locations in different regions (scenario (b)). In the semi-arid region, these models were tested in three new locations, namely KN, AN, and AK. Similarly, GLSN and GQSN models were tested with new data from different locations in the other regions, namely BJ (arid), JB, SM, BB, RC and RD (sub-humid), TR (humid). In this scenario (b), a behavior of the developed models similar to the one noticed under scenario (a) was observed, i.e., GLSN and GQSN with input combinations (ii) and (iv) performed better than the other combinations (i) and (iii). Therefore, the results pertaining to GLSN and GQSN models with input combinations (i) and (iii) are not shown in Table 7. The comparison of the results of GLSN and GQSN models showed that the performance of both models was comparable with slightly better performance of the GQSN models in all locations in every AER. Compared to GQSN models with the input combination (iv), the models which have T_{max}, T_{min}, and R_a as inputs showed superior performance. Therefore, under scenario (b), the superior performance of GQSN models with T_{max}, T_{min}, and R_a as inputs was observed in almost every location in all regions. This confirms the importance of R_a component as input during the development of HG based generalized models. Further, in Table 7, the performance of the HG method with respect to the FAO-56 PM prediction of ET_o is also displayed. The GLSN and GQSN models performed better than their conventional counterpart (HG) in all locations in every AER. These results suggest that both the GLSN and GQSN models are more accurate than the conventional method during the generalization testing as well.

4 Conclusions

The ability of GQSN models corresponding to HG method to estimate ET_o using pooled daily climate data from different locations in four AERs in India was studied in this paper. For the development of GQSN models, different input combinations were considered to assess the effect of each variable on the ANN estimated ET_o. The GQSN models were compared with the GLSN models. To test the accuracy of GQSN and GLSN models, their performance was also compared with the performance of the conventional HG and HG-C method against the FAO-56 PM method. The generalizing capability of the developed GQSN models was tested under two scenarios: (a) model development locations; and (b) model testing locations. The GLSN and GQSN models with the input combination (i) performed approximately 5, 10, and 20 % better compared to other combinations (ii, iii, and iv, respectively) for all AERs. Further, the GQSN models showed better performance when compared to GLSN models in all regions during model development. The developed GQSN and GLSN models performed much better than the corresponding conventional HG method. During testing of the generalizing capability of GQSN models for the above two scenarios, the GQSN models performed better than the GLSN models in all cases. Further, the GQSN and GLSN models with the input combinations

Table 7 Performance statistics of GLSN and GQSN models with model testing locations

Location	Performance	Models with the input combination				HG
		T_{max}, $T_{min,}$ and R_a		T_{max} and T_{min}		
		GLSN	GQSN	GLSN	GQSN	
Semi-arid						
KN	RMSE	0.855	0.843	0.992	0.990	1.058
	R^2	0.815	0.826	0.742	0.752	0.729
	RE	0.152	0.143	0.190	0.184	0.156
AN	RMSE	0.641	0.619	0.773	0.748	1.146
	R^2	0.817	0.831	0.730	0.746	0.702
	RE	0.116	0.109	0.150	0.142	0.191
AK	RMSE	1.097	0.838	1.160	1.159	1.519
	R^2	0.783	0.819	0.791	0.801	0.693
	RE	0.168	0.102	0.171	0.170	0.208
Arid						
BJ	RMSE	0.718	0.715	0.753	0.746	1.023
	R^2	0.702	0.713	0.668	0. 687	0.602
	RE	0.129	0.119	0.138	0.121	0.168
Sub-humid						
JB	RMSE	0.682	0.681	0.712	0.711	1.208
	R^2	0.856	0.862	0.838	0.838	0.745
	RE	0.128	0.116	0.135	0.135	0.217
SM	RMSE	0.702	0.692	0.809	0.808	0.942
	R^2	0.804	0.809	0.739	0.739	0.695
	RE	0.131	0.127	0.162	0.161	0.186
BB	RMSE	0.862	0.854	0.882	0.871	1.007
	R^2	0.737	0.740	0.639	0.686	0.612
	RE	0.159	0.154	0.156	0.143	0.175
RC	RMSE	0.574	0.571	0.617	0.603	1.277
	R^2	0.815	0.819	0.779	0.791	0.600
	RE	0.125	0.121	0.142	0.136	0.243
RD	RMSE	0.662	0.653	0.725	0.722	1.550
	R^2	0.833	0.837	0.799	0.800	0.786
	RE	0.151	0.144	0.181	0.182	0.305
Humid						
TR	RMSE	0.914	0.912	1.193	1.056	1.456
	R^2	0.489	0.512	0.481	0.485	0.406
	RE	0.165	0.164	0.176	0.158	0.170

(ii) and (iv) showed superior performance as compared to other combinations. The models with the input combination (i) and (iii) failed to show generalizing capability during both scenarios (a) and (b). Therefore, inclusion of altitude as an input may decrease the performance of generalized models during testing. The performance of generalized models was increased with the inclusion of latitude or Ra as an input during temperature-based ET_o modeling in

India. Overall, better performance of GLSN and GQSN models in comparison to HG and HG-C method in different AERs in India showed that these models not only have better potential but also have good generalizing capability. It may be noted that the main focus of this study was to evaluate the generalizing capability of quadratic neural networks in ET_o modeling. This study does not intend to replace the well established standard FAO-56 PM method. Further, more studies are required to test the generalizing capability of GQSN models with limited climate data for different climatic regions of other countries.

Acknowledgments The authors wish to thank All India Coordinated Research Project on Agro-meteorology (AICRPAM), Central Research Institute for Dryland Agriculture (CRIDA), Hyderabad, Andhra Pradesh, India for providing the requisite climate data to carry out this study. Also, the authors express their gratitude to the reviewers for useful comments and suggestions.

References

Adamala S, Raghuwanshi NS, Mishra A, Tiwari MK (2014a) Evapotranspiration modeling using second-order neural networks. J Hydrol Eng 19(6):1131–1140. doi:10.1061/(ASCE)HE.1943-5584.0000887

Adamala S, Raghuwanshi NS, Mishra A, Tiwari MK (2014b) Development of generalized higher-order synaptic neural based ET_o models for different agroecological regions in India. J Irrig Drain Eng. doi:10.1061/(ASCE)IR.1943-4774.0000784

Allen RG, Pereira LS, Raes D, Smith M (1998) Crop evapotranspiration: Guidelines for computing crop water requirements. FAO Irrigation and Drainage Paper no. 56 Rome Italy

Chakra NC, Song K-Y, Gupta MM, Saraf DN (2013) An innovative neural forecast of cumulative oil production from a petroleum reservoir employing higher-order neural networks (HONNs). J Pet Sci Eng. doi:10.1016/j.petrol

Chen JL, Li GS, Xiao BB, Wen ZF, Lv MQ, Chen CD, Jiang Y, Wang XX, Wu SJ (2015) Assessing the transferability of support vector machine model for estimation of global solar radiation from air temperature. Energy Convers Manag 89(1):318–329

El-Shafie A, Alsulami HM, Jahanbani H, Najah A (2013) Multi-lead ahead prediction model of reference evapotranspiration utilizing ANN with ensemble procedure. Stoch Env Res Risk A 27(6):1423–1440

Falamarzi Y, Palizdan N, Huang YF, Lee TS (2014) Estimating evapotranspiration from temperature and wind speed data using artificial and wavelet neural networks (WNNs). Agric Water Manag 140:26–36

Fisher JB, Malhi Y, de Araujo AC, Bonal D, Gamo M, Goulden ML, Hirano T, Huete AR, Kondo H, Kumagai T, Loescher H, Miller S, Nobre AD, Nouvellon Y, Oberbauer SF, Panuthai S, von Randow C, da Rocha HR, Roupsard O, Saleska S, Tanaka K, Tanaka N, Tu KP (2009) The land-atmosphere water flux in the tropics. Glob Chang Biol 15:2694–2714

Gupta MM, Jin L, Homma N (2003) Static and Dynamic Neural Networks: from Fundamentals to Advanced Theory. Wiley/IEEE Press, New York

Hargreaves GH, Samani ZA (1985) Reference crop evapotranspiration from temperature. Appl Eng Agric 1(2):96–99

Huo Z, Feng S, Kang S, Dai X (2012) Artificial neural network models for reference evapotranspiration in an arid area of northwest China. J Arid Environ 82:81–90

Jahanbani H, El-Shafie AH (2011) Application of artificial neural network in estimating monthly time series reference evapotranspiration with minimum and maximum temperatures. Paddy Water Environ 9(2):207–220

Kim S, Kim HS (2008) Neural networks and genetic algorithm approach for non-linear evaporation and evapotranspiration modelling. J Hydrol 351:299–317

Kisi O (2011) Modeling reference evapotranspiration using evolutionary neural networks. J Irrig Drain Eng 137:636–643

Kumar M, Raghuwanshi NS, Singh R, Wallender WW, Pruitt WO (2002) Estimating evapotranspiration using artificial neural network. J Irrig Drain Eng 128(4):224–233

Kumar M, Raghuwanshi NS, Singh R (2011) Artificial neural networks approach in evapotranspiration modeling: a review. Irrig Sci 29(1):11–25

Laaboudi A, Mouhouche B, Draoui B (2012) Neural network approach to reference evapotranspiration modeling from limited climatic data in arid regions. Int J Biometeorol 56:831–841

Landeras G, Ortiz-Barrredo A, Lopez JJ (2008) Comparison of artificial neural network models and empirical and semi-empirical equations for daily reference evapotranspiration estimation in Barque Country (Northen Spain). Agric Water Manag 95:553–565

Marti P, Gasque M (2010) Ancillary data supply strategies for improvement of temperature-based ANN models. Agric Water Manag 97:939–955

Marti P, Royuela A, Manzano J, Palau-Salvador G (2010) Generalization of ET_0 ANN models through data supplanting. J Irrig Drain Eng 136(3):161–174

Rahimikhoob A (2010) Estimation of evapotranspiration based on only air temperature data using artificial neural networks for a subtropical climate in Iran. Theor Appl Climatol 101:83–91

Redlapalli SK (2004) Development of neural units with higher-order synaptic operations and their applications to logic circuits and control problems. M.S. thesis Dept. of Mechanical Engineering University of Saskatchewan Saskatoon Canada

Shiri J, Nazemi AH, Sadraddini AA, Landeras G, Kisi O, Fard AF, Marti P (2013) Global cross-station assessment of neuro-fuzzy models for estimating daily reference evapotranspiration. J Hydrol 480:46–57

Shiri J, Sadraddini AA, Nazemi AH, Kisi O, Landeras G, Fard AF, Marti P (2014) Generalizability of gene expression programming-based approaches for estimating daily reference evapotranspiration in coastal stations of Iran. J Hydrol 508:1–11

Taylor JG, Commbes S (1993) Learning higher order correlations. Neural Netw 6(3):423–428

Tiwari MK, Song KY, Chatterjee C, Gupta MM (2012) River flow forecasting using higher-order neural networks. J Hydrol Eng 655–666. doi:10.1061/(ASCE)HE.1943-5584.0000486

Trajkovic S, Todorovic B, Stankovic M (2003) Forecasting reference evapotranspiration by artificial neural networks. J Irrig Drain Eng 129(6):454–457

Traore S, Wang YU, Kerh T (2010) Artificial neural network for modeling reference evapotranspiration complex process in Sudano-Sahelian zone. Agric Water Manag 97:707–714